Self-guided laser wakefield electron acceleration experiments on Astra Gemini – future prospects

S. P. D. Mangles, A. G. R. Thomas, L. Willingale, S. R. Nagel, C. Bellei, B. Dangor and Z. Najmudin
Blackett Laboratory, Imperial College London, London, SW7 2AZ, UK

Main contact email address **louise.willingale@imperial.ac.uk**

Abstract
Motivated by extensive experiments and simulations on the behaviour of laser wakefield accelerators with ~10 TW laser systems we investigate the extension of such experiments to the 500 TW regime that will be accessible using Astra Gemini. Using numerical simulations we identify the laser and target parameters that are most likely to result in a successful experiment, namely the laser focusing geometry, plasma densities and target lengths likely to result in a significantly increased energy electron-beam (> 1 GeV) without the use of external guiding structures.

Introduction
The field of laser driven electron acceleration has attracted significant international attention since the first observations of quasi-monoenergetic electron beams at the 15 TW Astra facility in 2003. Indeed since the first three reports on such experiments [1-3], there has been a surge in activity in the field. Results from both experiments (solid symbols) and particle-in-cell simulations [4-15] have been collated in figure 1.

The maximum energy and acceleration length required in a laser wakefield accelerator can be derived from simple considerations. The maximum length over which a wakefield can accelerate particles is governed by the dephasing length, that is the length over which a relativistic ($v \rightarrow c$) electron will overtake the plasma wave travelling at the group velocity of the laser pulse ($v_g = c(1\text{-}n_e/n_c)^{1/2}$) by half the wavelength of a relativistic plasma wave ($\lambda_p = 2\pi c/\omega_p$). n_e is the plasma density, $n_c = m\varepsilon_0\omega_0^2/e^2$ is the critical plasma density for electromagnetic wave propagation, where ω_0 is the laser frequency ($n_c = 1.75 \times 10^{21}$ cm^{-3} for 800 nm radiation). The dephasing length for $n_e << n_c$ is given by the formula [16]:

$$L_{dp} = \lambda_p \left(\frac{n_c}{n_e} \right) \qquad (1)$$

The maximum electron energy gain that a wakefield accelerator can produce can be estimated by integrating the electric field over a dephasing length (assuming a sinusoidal and the electric field amplitude. The electric field amplitude required to trap electrons that are initially at rest is given by:

$$E_0 = \frac{mc\omega_p}{e} \qquad (2)$$

(NB this is not the field at which 1D wave-breaking occurs ($E_{WB} = (2(\gamma_\phi - 1))^{1/2} E_0$) [17], where γ_ϕ is the Lorentz factor associated with the phase velocity of the plasma wave ($v_\phi \approx v_g$). E_{WB} is the electric field at which the plasma wave can trap and accelerate an electron initially moving at $-v_\phi$ to one moving at $+ v_\phi$ in the laboratory frame.)

This leads to an expression for the maximum energy an electron can gain from a plasma wave of amplitude E_0

$$W_{max} = 2mc^2 \left(\frac{n_c}{n_e} \right) \qquad (3)$$

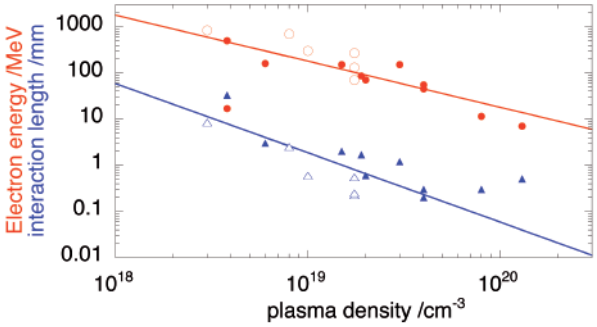

Figure 1. Collation of reported data from various experiments (solid symbols) and simulations (open symbols). Red symbols: Mono-energetic electron beam energy /MeV. Blue symbols: interaction length / mm. The solid lines correspond to expressions (1) and (3) in the text.

Equations (1) and (3) are also plotted on figure 1. It should be noted that this figure is on a log-log scale, so that any scatter from the theoretical curve appears diminished. Nevertheless the observed electron energies and interaction lengths follow these simple scaling laws remarkably well over a range of plasma densities. It should be noted that not all the data points are for similar laser systems. Data has been included from experiments with laser power as low as 2 TW and as high as 40 TW. Simulation data has been included for laser powers over the range 10 - 300 TW. Both experimental and simulation data presented includes self-guiding and external guiding channel results (from less than 1 mm to >10 mm).

This collection of data clearly shows the general trend that to increase the electron beam energy experiments must move to lower plasma density and longer interaction lengths. Stable 0.5 GeV acceleration has been achieved at LBNL following this approach, with some shots reaching the GeV level [9]. It should be noted that a more detailed scaling was proposed in [18] which states that the electron beam energy should increase with $n_e/(a_0 n_c)$, however the experimental data shown in figure 1 is over a fairly small range in a_0. The scaling proposed in [18] assumes the pulse duration is shorter than 'bubble' diameter (or plasma wavelength), which is not always the case for the presented data (particularly at high density).

We cannot simply reduce the plasma density to increase the electron beam energy; the laser parameters must also be altered so as to reach this mono-energetic regime. The self-similar behaviour of these accelerators with density requires that the pulse dimensions scale with √n while maintaining a minimum intensity; this requires the laser energy to increase with decreasing density. Tsung *et al.* [4] and Lu *et al.* [19] showed from simulations and analytical theory that for injection at the back of the first wave period a minimum intensity threshold of approximately $a_0 > 3$ is required. Experimental evidence to support this threshold was recently reported, assuming pulse compression and self-focusing in the plasma wave to a laser pulse with volume on the order of λ_p^3 [20].

While pulse evolution (i.e. self-focusing and pulse compression) has hitherto played a crucial role in reaching self-injection with 10-100TW lasers it has also been attributed to some of the remaining shot-to-shot variability of the electron beam parameters. An experimental study performed at Lund [20] has shown that the stability of the electron beam is increased when the pulse and plasma parameters are chosen such that the beam waist $w_0 \approx \lambda_p$, minimising self-focusing effects. It has also been experimentally verified that in this regime self-focusing tends to produce exit mode profiles with a beam waist approximately equal to the plasma wavelength [21] for laser powers above the critical power for self-focusing. 2D simulations also show that, for a range of plasma densities and focal geometries, self-focusing reduces the beam size until it is approximately $w_0 \approx \lambda_p$ after which stable propagation occurs. Figure 2 shows experimental and 2D Osiris simulation results that have been found to support this statement with 15 TW laser systems.

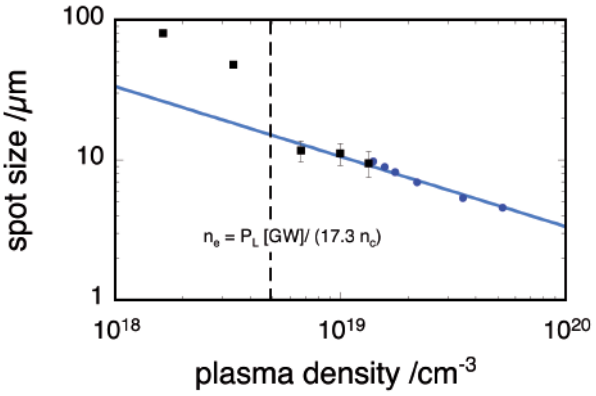

Figure 2. Results from a recent Astra 15 TW experiment (black squares) and 2D PIC simulations (blue circle) showing the dependence on the laser spot size (FWHM intensity ≈ 1/e² radius) with plasma density (experimental data taken from [21]). The blue curve shows the plasma wavelength λ_p. The black dotted line shows the density below which the laser in the experiment was below the critical power for self-focusing P_c [GW] = 17.3 (n_c/n_e).

A single beam of Astra Gemini is expected to produce a laser pulse of duration ≈30fs with pulse energy of ≈15 J on target. If we assume that the beam self-focuses to a matched spot size, $w_0 \approx \lambda_p$, and set a normalised intensity threshold for self-injection of $a_0 \approx 3$, as has been observed on 20 TW experiments then we can calculate a minimum plasma density at which we can expect to achieve electron injection in self-guided experiments on Gemini. The relationship between the laser pulse energy ε_L, pulse duration (FWHM) τ, and plasma density n_e can be found by comparing the power of the laser pulse:

$$P_L = \frac{m^2 c^3 \omega_0^2}{16 e^2} a_0^2 w_0^2 \tag{4}$$

and the critical power for self-focusing:

$$P_c = \frac{2 m^2 c^5}{e^2}\left(\frac{\omega_0^2}{\omega_p^2}\right) \approx 17.3\left(\frac{n_c}{n_e}\right)[\mathrm{GW}] \tag{5}$$

which produces:

$$\frac{P_L}{P_c} = \frac{\pi^2}{8}\frac{a_0^2 w_0^2}{\lambda_p^2} \tag{6}$$

Inserting the threshold vector potential required for trapping, a_t and using the fact that the peak laser power $P_L \approx 0.9\,\varepsilon_L/\tau$

$$\frac{\varepsilon_L}{[\mathrm{J}]} = 23.3 \times 10^9 \left(\frac{n_c}{n_e}\right) a_t^2 \frac{\tau}{[\mathrm{s}]} \tag{7}$$

Equation (7) does not include the effects of pulse compression and frequency shifting of the pulse spectrum. For low plasma densities and short laser pulses (when $c\tau < \lambda_p/2$) we can reasonably expect the pulse compression to be minimal, therefore we can use equation (7) to predict the minimum density at which a laser pulse containing ε_L will be able to drive a wake to self-injection. Equation (7) is shown as a function of plasma density for τ = 30 fs in figure 3. For a laser energy of 10 J we expect the minimum density at which self-injection will occur will be ≈ 1×10^{18} cm^{-3} and that the corresponding electron energy will be $W \approx$ 1.5 - 2 GeV. To achieve early injection

Simulation number	Density / cm^{-3}	Vacuum beam waist, w_0 (1/e² intensity radius)/μm	Vacuum Rayleigh range, Z_R/mm	Peak normalised vector potential, a_0
1	1.05×10^{18}	5	0.1	18.8
2	1.05×10^{18}	10	0.4	9.6
3	1.05×10^{18}	20	1.6	4.8
4	1.05×10^{18}	34	4.5	2.8
5	2.10×10^{18}	20	1.6	4.8

Table 1. Physical parameters used for the simulations presented, the simulation numbers are used throughout the report. The laser pulse duration was 30 fs (FWHM) and the pulse energy was 10 J for all the simulations.

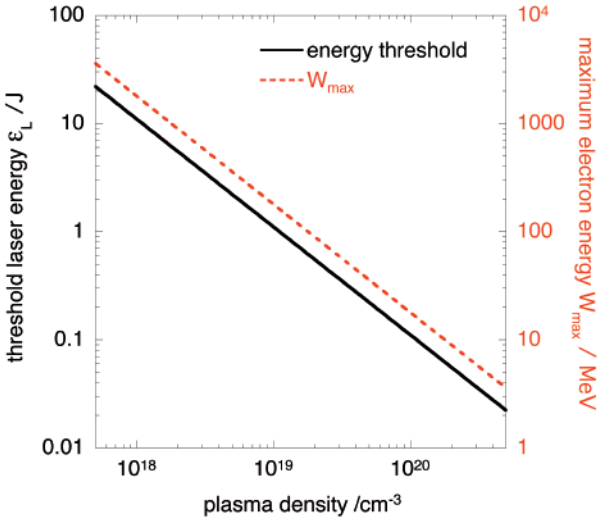

Figure 3. Threshold laser energy, ε_L, required to reach self-injection as a function of plasma density (solid line, left axis) and corresponding electron energy W_{max} (dashed line, right axis).

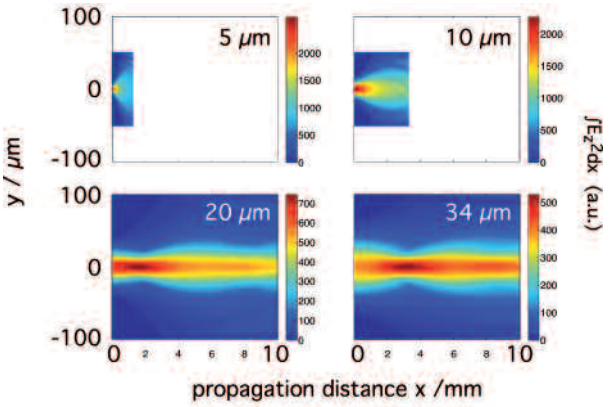

Figure 4. Evolution of the transverse laser pulse envelope at a plasma density of n_e = 1 (10^{18} cm^{-3} for various beam waists. Simulations 1-4 are shown. The transverse size of simulations 3 and 4 was increased to 200 μm compared to 100 μm for simulations 1 and 2.

(maximising the available acceleration length) and minimise instabilities associated with self-focusing we therefore expect a focal spot size on the order of $w_0 \approx \lambda_p \approx 34$ μm to be the most efficient and we use these parameters as the starting point of our simulations.

Numerical modelling of Gemini electron acceleration experiments

A series of simulations investigating electron acceleration experiments on Astra Gemini have been carried out. The simulations were performed using the particle in cell code Osiris [22] in 2D3V slab geometry. In these runs the laser propagates in the x direction, the slab lies in the x-y plane and the fields and particle momenta have components in x, y and z. The laser was polarized in the y-z plane. We use stationary ions. The simulations were performed on the 48 node "Caesar" cluster at Imperial College. The simulation resolution was carefully chosen to minimise numerical dispersion errors while maintaining an acceptable run size. Typical run parameters were $\Delta x = 0.2\ c/\omega_0$; $\Delta y = 0.8\ c/\omega_0$; $\Delta t = 0.199\ 1/\omega_0$ in a simulation box size of up to $1600 \times 1600\ c/\omega_0 \approx 200 \times 200$ μm. The simulation box moves in the direction of the laser propagation at the speed of light. The simulations were performed with a stationary ion background. The longest runs performed were for propagation distances as large as 1 cm. The physical parameters of the runs presented in this report are shown in table 1.

Figure 4 shows the evolution of the laser electric field envelope in simulations 1 - 4. Each vertical slice in the image corresponds to the transverse profile of the laser envelope after integration along the propagation direction (x). The four simulations shown in figure 4 were all performed with a bulk plasma density of $n_e = 1 \times 10^{18}$ cm^{-3} but with varying focal geometries (characterised by the vacuum beam waist w_0). For small spot sizes, w_0 = 5 and 10 μm, which correspond to $w_0 < \lambda_p$, the pulse clearly diverges and is not significantly self-guided, indeed these simulations were halted after 2 and 4 mm propagation due to interaction of the diffracting pulse with the box boundary. As the spot size becomes close to the plasma wavelength significant guiding is observed. For w_0 = 20 and 34 μm there is still significant laser intensity after a propagation distance of 1 cm. The w_0 = 34 μm simulation has guided over approximately $2Z_R$, which might not be considered as extensive guiding ($Z_R = \pi w_0^2/\lambda$ is the Rayleigh range). However the w_0 = 20 μm case has guided for over $6Z_R$. In this case self-guiding is due to the transverse density profile of the plasma wave.

Self-guiding alone is insufficient to produce an electron beam. The self-guided pulse must maintain a sufficiently high intensity to produce self-injection. In the following we concentrate on self-injection in the first wave period since it is known that 2D simulations can over estimate self-injection in the trailing periods compared with full 3D runs [23]. In figure 5 we show the electron density distribution of the first plasma wave period from three simulations (numbers 4,3 and 5 in table 1) after the laser has propagated for 9.6 mm. In these plots the laser propagation direction is left to right. Simulation 4, at a density of $n_e = 1 \times 10^{18}$ cm^{-3} and a spot size matched to the plasma wavelength λ_p has not injected in the first period even at this late stage. In simulation 4, $a_0 = 2.8$, which is close to, but just below, the expected threshold for injection ($a_t \approx 3$). Pulse modification would be required before injection could occur, however as the pulse waist is already matched to λ_p and the pulse length ($c\tau$ = 9 μm) is less than $\lambda_p/2$ we might expect minimal self-focusing and compression. Simulation 3, also at a density of $n_e = 1 \times 10^{18}$ cm^{-3} has also failed to produce self-injection in the first period. In this case $a_0 = 4.8$ which is above the expected threshold. This failure is explained by the fact that the pulse diffracts slightly since $w_0 < \lambda_p$, reducing the intensity before the plasma wave reached a sufficiently high amplitude. Simulation 5 shows the effect of moving to a higher plasma density ($n_e = 2 \times 10^{18}$ cm^{-3}), while maintaining the spot size of simulation 3. In this case the plasma wavelength is λ_p = 23 μm which is very close to the spot size w_0 = 20 μm, hence sufficient laser energy is trapped in the first plasma wave period and the intensity is high enough to cause self-injection after 4.2 mm propagation. The electron density plot shown here is after 9.6 mm of propagation, and shows an electron bunch that has been accelerated for over 5 mm.

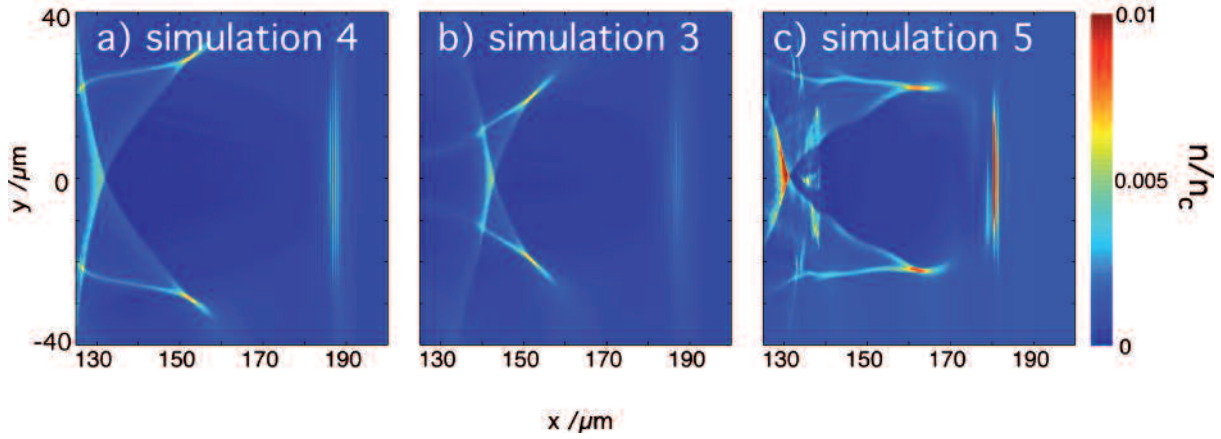

Figure 5. Electron density profile after 9.6 mm propagation from three simulations investigating injection threshold. The left panel is simulation 4. The middle panel is simulation 3, and the right panel is simulation 5.

Figure 6 shows the accelerating field at the point where injection has just occurred. The peak accelerating field is close to $E_x = 5\ mc\omega_p/e = 0.7$ GeV/mm. We therefore expect that, if this field were maintained over the entire acceleration length of 5 mm then electron energies close to 3 GeV would be obtained. This electric field at the back of the bubble is above the trapping threshold for stationary electrons, E_0, but is significantly less than the 1D cold wavebreaking field for this plasma density, $E_{WB} \approx 40\ E_0$, indicating that multi-dimensional effects are significant in determining the exact electron trajectories. That the field in the bubble is significantly larger than E_0 is somewhat at odds with the scaling presented in figure 1. Using that scaling we would predict peak electron energies of 0.85 GeV at the plasma density of simulation 5 ($n_e = 2 \times 10^{18}$ cm^{-3}).

An electron spectrum calculated from simulation 5, considering only electrons that would pass through an electron spectrometer with a 25 mrad acceptance cone (corresponding approximately to the electron spectrometer that will be used in the first experiments on Astra Gemini) is shown in figure 7. This shows a quasi-mononenergetic spectrum at approximately 2 GeV (2% relative energy spread). We note that in this case the maximum energy is close to $W_{max} \approx 2\ a_0\ mc^2\ (n_c/n_e)$. which is consistent with scalings including the dependence on a_0 [18,19].

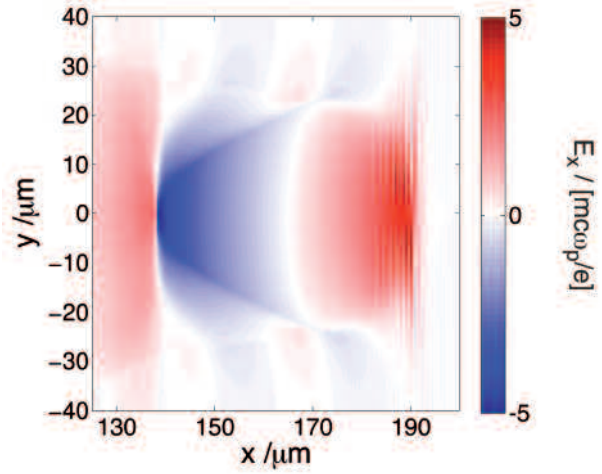

Figure 6. Longitudinal electric field (E_x) of the first plasma wave period in simulation 5 after 4.2 mm propagation. Blue (red) regions correspond to accelerating (decelerating) fields. The normalisation corresponds to $E_x = 5\ mc\omega_p/e = 0.7$ GV/mm.

Summary

In a series of particle-in-cell simulations we have investigated the parameters of interest for the forthcoming Astra Gemini experiments on self-guided laser wakefield acceleration. Using simple scaling laws we identified the regions of interest and have then verified and refined these using 2D PIC simulations. We have considered the appropriate focusing geometry and plasma target requirements necessary to produce quasi-monoenergetic electron beams to the multi-GeV level. The simulations show that a focal spot size on the order of 20 μm (i.e. f/20 focusing) is ideal and that plasma targets of centimetre length capable of producing densities up to a few 10^{18} cm^{-3} are suitable. Such targets have been developed and fielded on an experimental campaign at LULI where guiding of a 300 fs, 30 J pulse was observed over 1 cm with f/20 focusing [24]. Although the longer pulse duration in the LULI experiments ($c\tau > \lambda_p/2$) means that relativistic self-guiding was significant, as opposed to the guiding due to electron expulsion that is dominant in the bubble regime, this result still indicates the suitability of these targets for the forthcoming experiments and indicates that multi-GeV

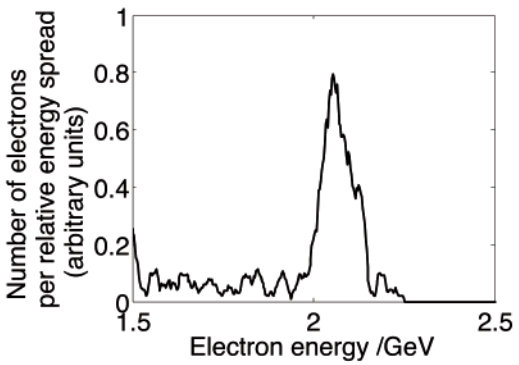

Figure 7. Electron energy spectrum (number of electrons per relative energy spread) after 9.6 mm propagation in simulation 5. The electron spectrum is calculated for electrons travelling within a cone angle of 25 mrad. The FWHM energy width of this beam is ≈ 2%.

beams from a self-guided wakefield accelerator should be experimentally realisable in the near future.

References

1. S. P. D. Mangles *et al., Nature,* **431**, 535 (2004).
2. C. G. R. Geddes *et al., Nature,* **431**, 538 (2004).
3. J. Faure *et al., Nature,* **431**, 541 (2004).
4. F. S. Tsung *et al., Phys. Rev. Lett.,* **93**, 185002 (2004).
5. S. A. Reed *et al., Appl. Phys. Lett.,* **89**, 231107 (2006).
6. A. Pukhov and J. Meyer-ter-Vehn, *Appl. Phys. B*, **74**, 355 (2002).
7. E. Miura *et al., Appl. Phys. Lett.,* **86**, 251501 (2005).
8. S. P. D. Mangles *et al., Phys. Rev. Lett.,* **96**, 215001 (2006).
9. W. P. Leemans *et al., Nat. Phys.,* **2**, 696 (2006).
10. H. Kotaki *et al., Laser Physics,* **16**, 1107 (2006).
11. C. T. Hsieh *et al., Phys. Rev. Lett.,* **96**, 095001 (2006).
12. T. Hosokai *et al., Phys. Rev. E,* **73**, 036407 (2006).
13. B. Hidding *et al., Phys. Rev. Lett.,* **96**, 105004 (2006).
14. N. Hafz *et al., Nucl. Intrs. Methods A*, **554**, 49 (2005).
15. M. Geissler, J. Schreiber and J. Meyer-Ter-Vehn, *New J. Physics,* **8**, (2006).
16. E. Esarey *et al., IEEE Trans. Plasma Sci.,* **24**, 252 (1996).
17. A. Akhiezer and R. Polovin, *JETP,* **3**, 696 (1956).
18. S. Gordienko and A. Pukhov, *Phys. Plasma,* **12**, 043109 (2005).
19. W. Lu *et al., Phys. Plasma,* **13**, 056709 (2006).
20. S. P. D. Mangles *et al., Phys. Plasma,* **14**, 056702 (2007).
21. A. G. R. Thomas *et al*., *Phys. Rev. Lett*., **98**, 095004 (2007).
22. R. A. Fonseca *et al*., in Lecture Notes in Computer Science. 2002, Springer: Heidelber. p. 342.
23. F. S. Tsung, private communication, (2006).
24. C. Kamperidis, private communication, (2006).